2008

Kinetics of spinel formation and growth during dissolution of MgO in CaO-Al2O3-SiO2 slag

Sharon Nightingale
University of Wollongong, sharon@uow.edu.au

B. J. Monaghan
University of Wollongong - Dubai Campus, monaghan@uow.edu.au

Communication

Kinetics of Spinel Formation and Growth during Dissolution of MgO in $CaO-Al_2O_3-SiO_2$ Slag

S.A. NIGHTINGALE and B.J. MONAGHAN

The formation and growth of $MgAl_2O_4$ spinel crystals on a single-crystal MgO substrate submerged in a 40 pct CaO, 40 pct SiO_2, and 20 pct Al_2O_3 slag were directly observed using high-temperature microscopy. This showed that the crystals initially form on the MgO surface, but may break off and be carried out into the liquid slag. Still pictures extracted from digitally recorded images were used to measure the size of these crystals at 1420 °C, 1440 °C, and 1460 °C as a function of time. Growth of the crystals was found to follow the parabolic rate law, with rates increasing with temperature. An activation energy of 564 kJ mol^{-1} was estimated from the experimental data. This was found to be comparable with previously published results from different types of experiments on spinel formation.

DOI: 10.1007/s11663-008-9186-y

During metallurgical processing, the formation of a spinel layer is desirable as it can protect the MgO refractory from further degradation. However, to do this, the spinel must quickly form a coherent layer that remains attached to the MgO. Therefore, the kinetics of spinel formation and morphology of its growth are of significant interest.

During dissolution of MgO immersed in molten slags containing Al_2O_3, various researchers have found that a spinel ($MgAl_2O_4$) layer may form at or near the MgO surface under both static and dynamic flow conditions.[1–6] Evidence from quenched samples has suggested that the spinel forms at the liquid/solid interface, but then often becomes detached from the solid unless anchored by protrusions on the solid MgO surface. Therefore, this layer can be easily removed by forced liquid flow. Similar observations were made during studies of indirect dissolution of alumina-based materials in contact with a variety of slag types by Sandhage and Yurek.[7]

In-situ observation of MgO dissolution has confirmed the formation of spinel, but as the focus of the study was inclusion dissolution, the location of initial formation was not observed.[8] A second study using high-temperature microscopy designed to observe indirect dissolution of MgO refractory in $CaO-Al_2O_3-SiO_2$ slags found that spinel crystals formed quickly at the interface. However, significant liquid flow occurred during the experiment, and the spinel crystals broke away from the interface and were quickly carried out into the slag.[9] Visibility of the crystals was obscured by the coarse-grained, opaque nature of the refractory grade material limiting the information that could be extracted from these experiments.

In this study, high-temperature microscopy was used to directly observe the formation and growth of spinel crystals on a single-crystal MgO substrate and the kinetics of crystal growth measured over a range of temperatures. The transparent nature of the substrate resulted in excellent visibility of the crystals so that it was possible to measure crystal size. The technique used also allowed observation of the detachment of the crystals from the substrate.

The slag was prepared by mixing and premelting appropriate mixtures of laboratory grade oxide powders in a platinum crucible at 1550 °C, quenching the fused slag and then crushing the resultant glass. This process was repeated to obtain a homogenous slag. The slag comprised 40 pct CaO, 40 pct SiO_2, and 20 pct Al_2O_3. The slag composition was selected to allow spinel formation and to ensure that the slag was transparent to the imaging system. The slag composition was confirmed using an inductively coupled plasma fusion technique.

Powdered slag was then packed into 5-mm-diameter Pt crucibles, melted at 1450 °C, and then quenched. The slag was inspected using an optical microscope to ensure that it was free of crystalline material prior to the experiment.

Thin slices (1-mm thick) of MgO were cut from single crystals and the surface polished using diamond media to a 9-μm finish. This slice was then divided into small pieces approximately 2×3 mm. One piece of MgO was then placed on top of the cold slag in the Pt crucible. The weights of the slag and MgO were recorded. The mass ratio of slag to MgO was approximately 7. The MgO single crystal was supplied by QMAG (Toowong, Australia).

The prepared sample was then placed in an infrared furnace attached to an optical microscope with a digital recording system (Figure 1). Samples were heated in air at 100 °C/min to 1420 °C, 1440 °C, or 1460 °C and then held at the desired temperature while crystal growth was observed. Images were recorded directly to a computer in digital format at 30 frames/s. At least two separate experiments were done at each hold temperature. The temperatures quoted have been corrected to account for the remote position of the thermocouple and have an estimated uncertainty of ±6 °C.

Still pictures were extracted from the video recordings at approximately 10-second intervals. The time at which a crystal first became visible was defined as time zero. The individual crystal size was determined by measuring the lengths of the sides of the base of the crystal, and the average was calculated. Spatial measurements in both vertical and horizontal directions were calibrated using an E. Leitz Wetzlar graticule. Only crystals that were

S.A. NIGHTINGALE, Professor, and B.J. MONAGHAN, Pyrometallurgical Group leader, are with the Faculty of Engineering, School of Mechanical Materials and Mechatronics, Materials Engineering, University of Wollongong, Wollongong, NSW 2522, Australia. Contact e-mail: monaghan@uow.edu.au

Manuscript submitted May 29, 2008.
Article published online October 3, 2008.

clearly in focus and did not overlap with other crystals were measured. These measurements were then used to estimate growth rates and activation energy, as explained subsequently.

The MgO substrate sank beneath the surface of the liquid slag as the temperature increased. The first crystals became visible within seconds of submersion.

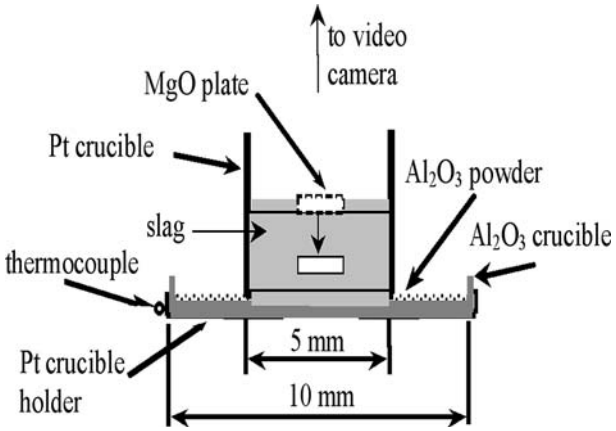

Fig. 1—Schematic diagram of test arrangement.

A typical sequence of micrographs taken from the video recordings of crystal growth is shown in Figure 2. As Figure 2 shows, the crystals have a well-developed faceted morphology, displaying the octahedral form typical of a cubic crystal bounded by (111) planes. This same morphology was observed in all experiments.

As the experiments progressed, some dissolution of the crystals was observed, and some crystals began to overlap. No further measurements of size were taken from crystals once either of these phenomena was observed. Results of the measurements of the size of the crystals as a function of time are shown in Figure 4.

A phase diagram of the system studied was constructed using MTDATA*[10] (Figures 3 and 4). This predicts that $MgAl_2O_4$ would be expected to form under the experimental conditions, and the morphology of the crystals is consistent with this. One sample from a similar experiment was quenched, sectioned, and polished for

*MTDATA is a commercial thermodynamic software package developed at the National Physical Laboratory in the United Kingdom, which is able calculate complex multicomponent phase equilibria in gas-liquid-solid systems. It uses a Gibbs energy minimization routine to establish the thermodynamic equilibrium of a defined system.

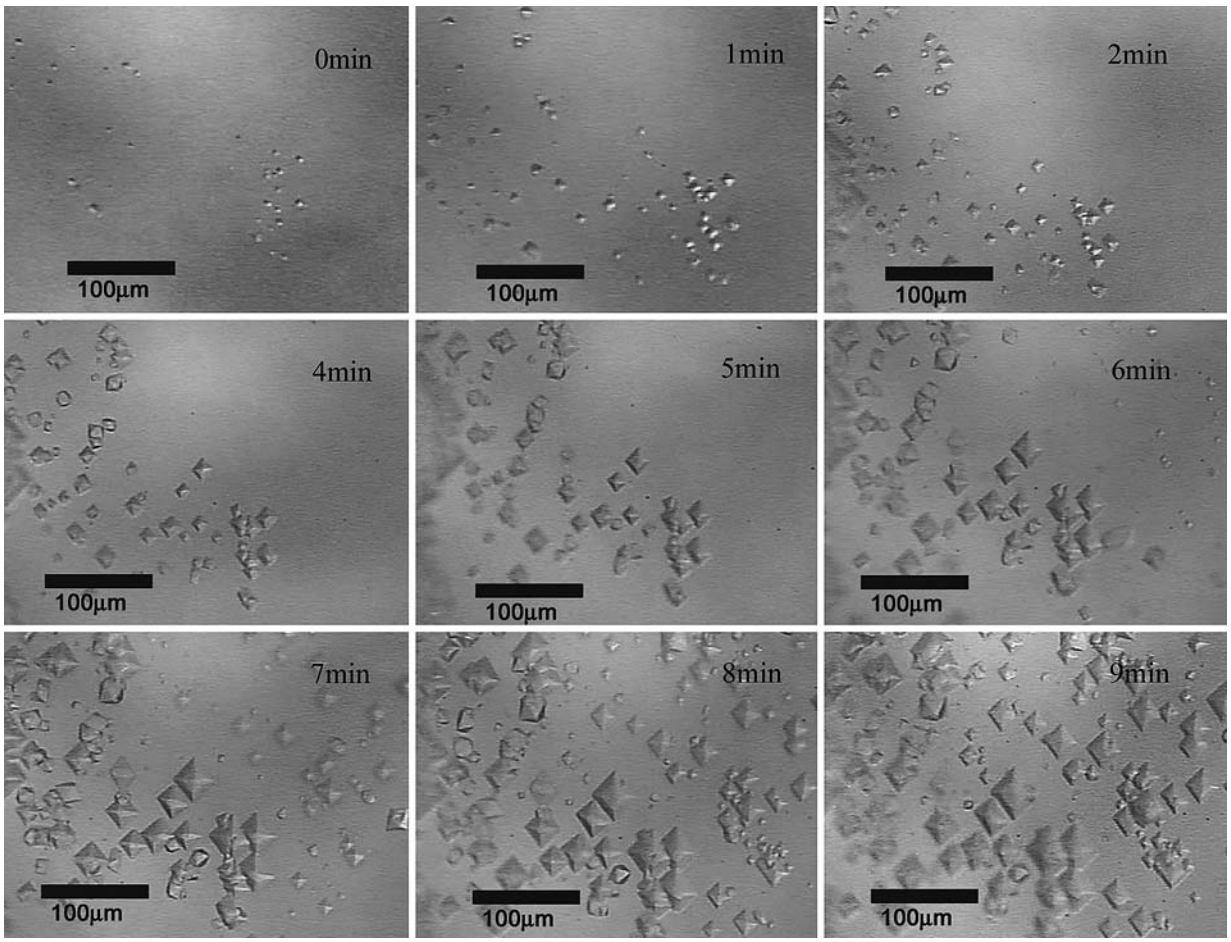

Fig. 2—Still images taken from digital video recordings of growth of spinel crystals on MgO substrate submerged in CAS slag at 1460 °C.

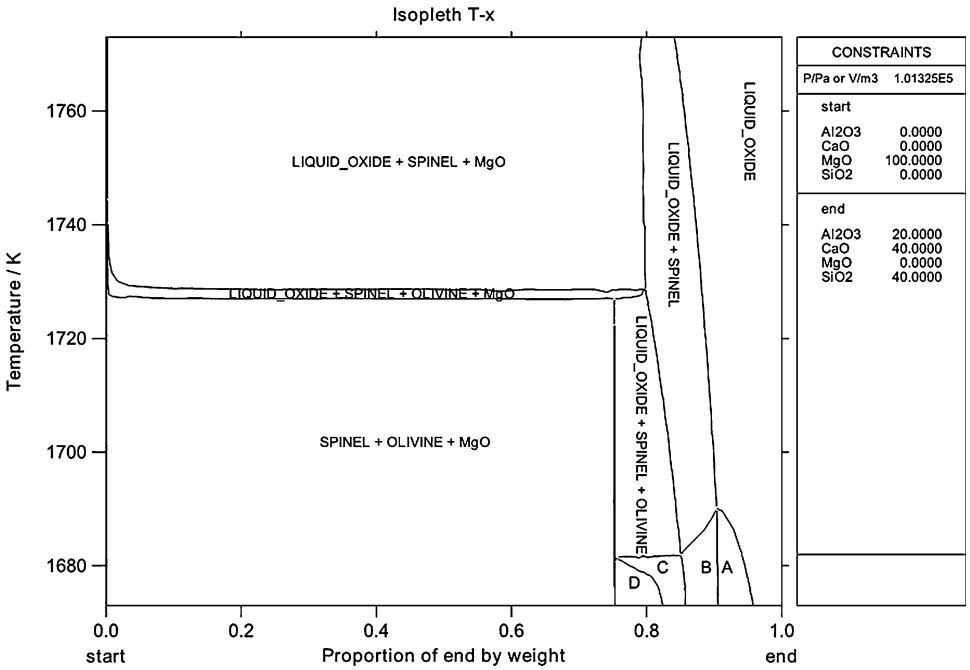

Fig. 3—Equilibrium phase stability for the MgO-slag system. "Start" is 100 pct MgO, and "end" is 100 pct experimental slag. The phase fields denoted A, B, C, and D contain phases liquid oxide + melilite, liquid oxide + melilite + spinel, liquid oxide + melilite + spinel + olivine, and melilite + spinel + olivine, respectively. Due to the scale used in this diagram, the MgO phase field at the MgO-rich end of the diagram cannot be resolved.

examination in the scanning electron microscope. The EDS analysis of the crystals yielded a composition of 74 pct Al_2O_3 and 26 pct MgO, confirming that the crystals are spinel. The EDS analyses under conditions used are estimated to be approximately ±5 pct.

To assess whether the formation of the spinel crystals significantly changes, the slag composition, the mass change of the slag during the experiments, was estimated. The mass change in 0.1 g of slag when 1000 of the largest sized spinel crystal measured in this study are formed was found to be less than 0.08 pct. The density of spinel was assumed to be 23,000 mol·m^{-3} for this calculation and based on previous work by Monaghan *et al.*[11] on spinel at 1500 °C. Given this small change in slag weight, it is assumed that the slag composition is effectively constant throughout the experiment.

The kinetics of formation of a reaction product on a surface is commonly analyzed by considering the counterdiffusion of cations through a layer. A schematic showing the growth of a spinel ($MgAl_2O_4$) layer on MgO is given in Figure 5. Growth of the product layer can be represented by the parabolic rate law[12] given in Eq. [1]:

$$\int_0^x x\,dx = \int_0^t k\,dt \qquad [1]$$

and

$$x^2 = 2kt \qquad [2]$$

where x is the thickness of the spinel ($MgAl_2O_4$) layer in μm, k is the parabolic rate constant with units $\mu m^2\ s^{-1}$, and t is the time in seconds.

This model is not directly applicable to these experiments, because it considers the formation of a layer of uniform thickness, and not specifically the growth of pyramidal crystals. To facilitate its use, the following approach has been adopted.

The base length (a) of the pyramid, as measured in the experiments, has been used to calculate the pyramid height and volume. Because the spinel $MgAl_2O_4$ is an AB_2X_4 structure type, where A and B represent two different cations and X represents the anion,[13] the height (h) and volume (V) can be calculated from Eqs. [3] and [4].

$$h = \frac{a}{\sqrt{2}} \qquad [3]$$

$$V = \frac{1}{3}\,a^2 h \qquad [4]$$

From this volume (V), an effective layer thickness (x') was calculated using Eq. [5], assuming that this volume represented a cuboid with a square base of length a.

$$x' = \frac{V}{a^2} \qquad [5]$$

Equation [2], the parabolic rate equation, was evaluated using the effective layer thickness x' calculated from the experimental spinel growth data and plotted in Figure 6. The solid line represents linear regressions of the data. Regression equations and their R^2 values are also given in the figure. For a given temperature, each data point represents an average of all experimental runs shown in Figure 4 at a given time.

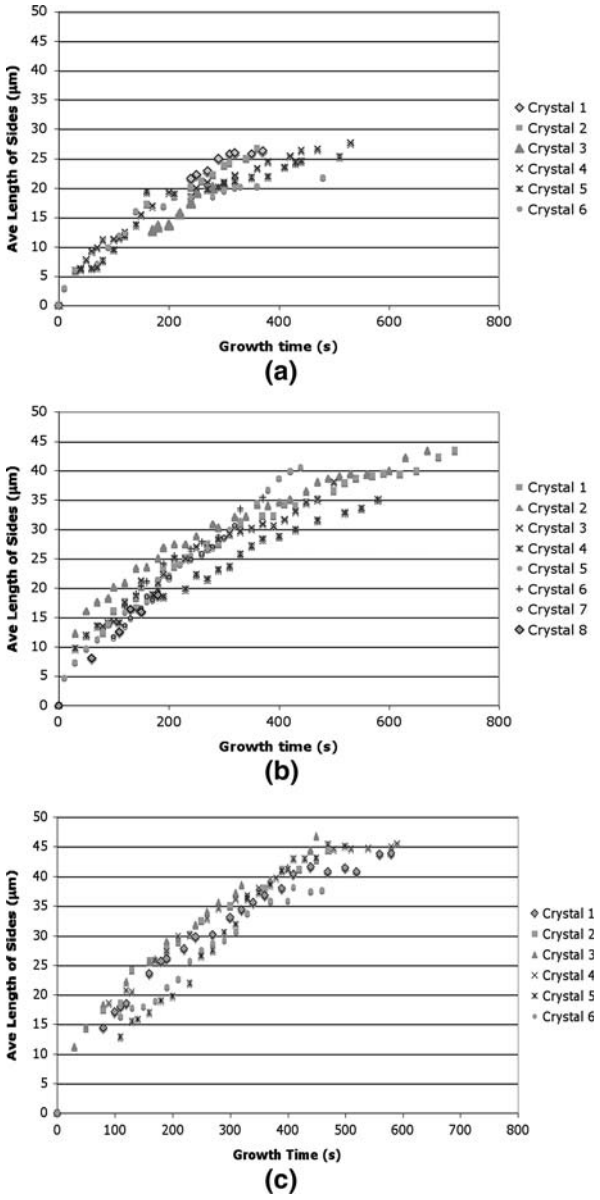

Fig. 4—Crystal size as a function of time at (*a*) 1420 °C, (*b*) 1440 °C, and (*c*) 1460 °C.

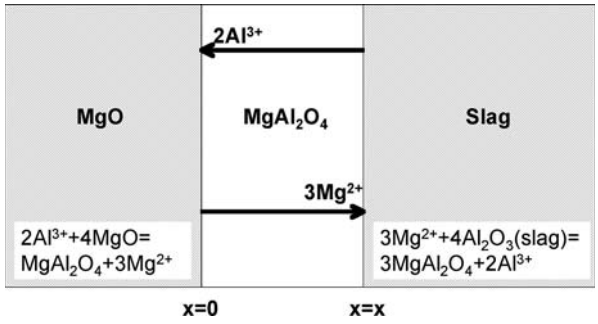

Fig. 5—Schematic showing the growth of a spinel ($MgAl_2O_4$) on MgO.

From Figure 6, it can be seen that a plot of the square of the effective layer thickness *vs* time is linear and that increasing temperature increases the rate of growth of

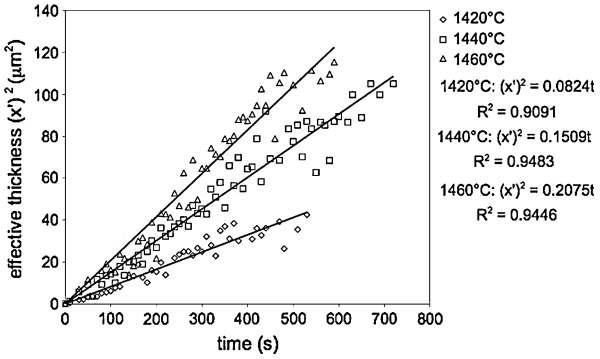

Fig. 6—A plot of x'^2 *vs* time for the experimental data. The solid lines and the associated equations represent linear regressions of the data.

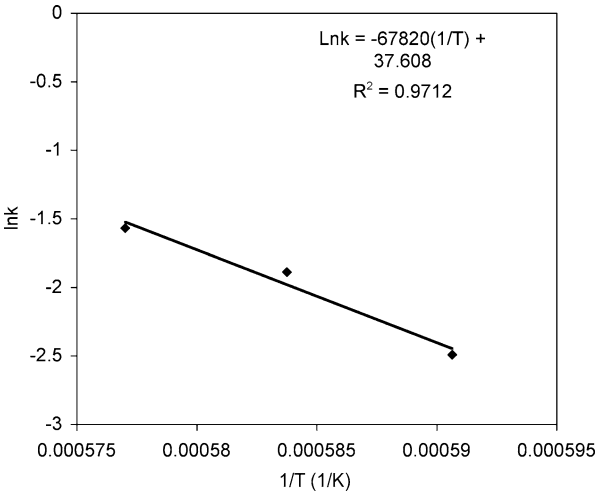

Fig. 7—An Arrhenius plot for the parabolic rate constant k.

the layer. Further, the high R^2 value (>0.9) for the linear regression lines indicates that the lines are a good fit to the experimental data.

The linear relationship between x'^2 and time is consistent with what is expected from the parabolic rate expression given in Eq. [2], indicating that the growth of the spinel crystals is parabolic. An explanation of the effects of temperature on the spinel growth can be found by considering the effects of temperature on k. The k value in Eq. [2] has an Arrhenius relationship with temperature, as shown in Eq. [7]:[12]

$$k = k_o e^{-E/(RT)} \qquad [7]$$

where k_o is a pre-exponential constant, E is an activation energy, R is the gas constant, and T is temperature. From Eq. [7], it can be seen that increasing temperatures increases k exponentially. This, in turn, results in an increase in the growth rate of the spinel. The Arrhenius relationship k with temperature relates to the mobility of the diffusing ions in the spinel layer.[12] The k_o constant and activation energy E from Eq. [7] were evaluated graphically from an Arrhenius plot (Figure 7) and found to be 2.15×10^{16} μm^2 s^{-1} and 564 kJ mol^{-1}, respectively.

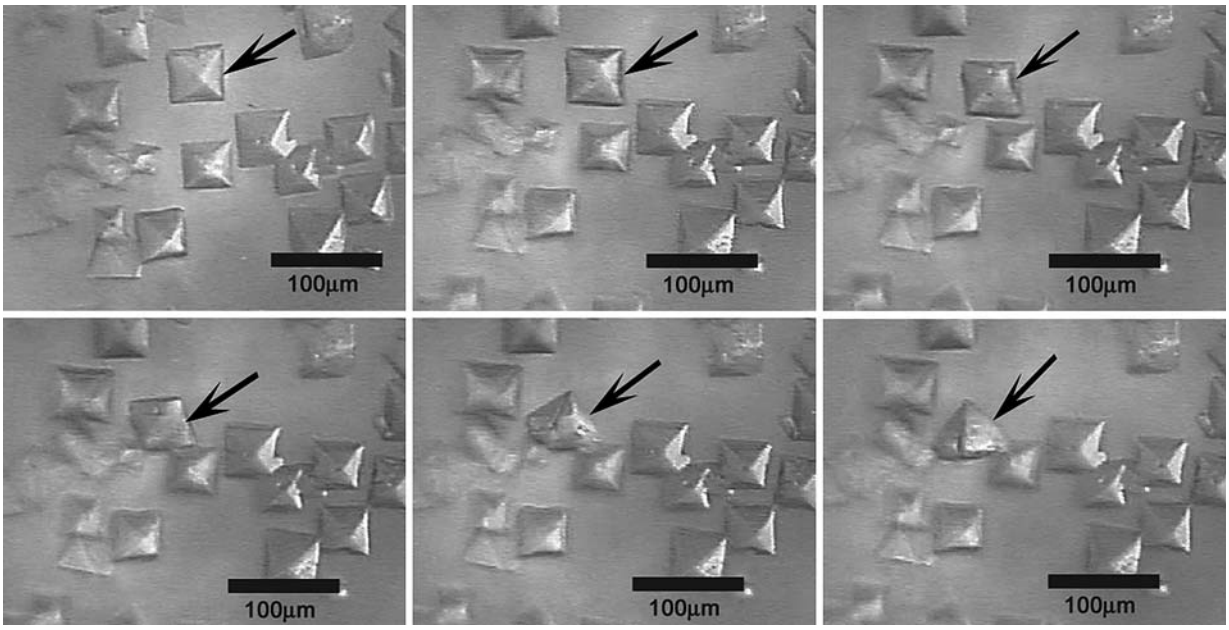

Fig. 8—A sequence of still images showing one crystal (marked by an arrow) detaching from the substrate and moving away from the original location. Frames are taken at 2- to 3-s intervals from an experiment performed at 1440 °C. The crystal rotated as it moved, providing a side view. This allowed the height of the crystal to be measured.

Given that these values have been obtained from a regression fit to three data points, they should be considered as indicative only. Though these values can only be considered indicative, the activation energy calculated for these experiments is comparable with a value of 401 kJ mol^{-1} for the Mg^{2+} diffusion coefficient in a spinel ($MgAl_2O_4$) obtained from high-temperature (1200 °C to 1400 °C) diffusion data reported in Kofstad[14] and 419 kJ mol^{-1} reported by Navais.[15]

From this investigation, little can be stated about the diffusing cations Mg^{2+} and Al^{3+}. The diffusion coefficient of these ions is inversely proportional to their ionic radii.[12] Therefore, given that their respective ionic radii are 0.072 and 0.053 nm,[13] it would be expected that the larger Mg^{2+} ion would have a lower mobility in the spinel layer. Though not indicated in Figure 5, there is the possibility of O^{2-} migration. However, given its large size, 0.140 nm,[13] relative to Mg^{2+} and Al^{3+}, this is considered unlikely.

It was also noted that crystals would spontaneously detach from the substrate and move away from their original location. Figure 8 provides a sequence of pictures illustrating this process for one crystal. Rotation of this crystal provided a side view, allowing the height to be measured. The measured height was found to be consistent with the cubic structure. In many cases, the crystals drifted well out into the liquid phase. This is in agreement with observations made during dissolution of polycrystalline MgO.[6,9]

There is a large volume change associated with the transformation from MgO to $MgAl_2O_4$. The lattice parameter of the spinel (0.808 nm)[16] is almost double that of MgO (0.421 nm),[17] resulting in significant mismatch and strain at the interface, which could lead to fracture and detachment of the spinel crystals.

Direct observations made using high-temperature microscopy confirm that $MgAl_2O_4$ spinel crystals form and grow on the MgO/slag interface. Crystal growth follows the parabolic rate law, with growth rate increasing as a function of temperature. The large difference in lattice parameters between MgO and $MgAl_2O_4$ leads to significant strain at the interface, resulting in fracture of some crystals and movement out into the slag. An activation energy of 564 kJ mol^{-1} estimated from the experimental data was in good agreement with data published by other authors using different techniques.

The authors thank Mark Reid and David Richards for their valuable contributions to the experimental work.

REFERENCES

1. K. Goto, B.B. Argent, and W.E. Lee: *J. Am. Ceram. Soc.*, 1997, vol. 80 (2), pp. 461–67.
2. R. Rait: Ph.D. Thesis, University of Melbourne, Melbourne, Australia, 1997.
3. T. Tran, S. Nightingale, and G. Brooks: *J. Aust. Ceram. Soc.*, 1998, vol. 34, pp. 33–38.
4. B.J. Monaghan, S.A. Nightingale, L. Chen, and G.A. Brooks: *Proc. VII Int. Conf. on Molten Slags, Fluxes and Salts*, Cape Town, South Africa, Jan. 25–28, 2004, pp. 598–607.
5. Y. Chen, G.A. Brooks, and S.A. Nightingale: *Can. Metall. Q.*, 2005, vol. 44 (3), pp. 323–29.
6. S.A. Nightingale, G.A. Brooks, and B.J. Monaghan: *Metall. Mater. Trans. B*, 2005, vol. 36B, pp. 453–61.
7. K.H. Sandhage and G.J. Yurek: *J. Am. Ceram. Soc.*, 1988, vol. 71 (6), pp. 478–89.

8. M. Valdez, K. Prapakorn, A.W. Cramb, and S. Sridhar: *Steel Res.*, 2001, vol. 72, pp. 291–97.
9. S.A. Nightingale and B.J. Monaghan: *Proc. Austceram & 3rd Int. Conf. on Advanced Materials Processing*, Melbourne, Australia, Nov. 30–Dec. 3, 2004, pp. 130–31.
10. R.H. Davies, A.T. Dinsdale, J.A. Gisby, S.M. Hodson, and R.G.J. Ball: *Conf. Applications Thermodynamics on the Synthesis and Processing of Materials*, Rosemont, IL, 1994, ASM/TMS, Warrendale, PA, pp. 371–84.
11. B.J. Monaghan and L. Chen: *Ironmaking and Steelmaking*, 2006, vol. 33, pp. 323–30.
12. D.R. Poirier and G.H. Geiger: *Transport Phenomena in Materials Processing*, TMS, Warrendale, PA, 1994, pp. 444–93.
13. W.D. Callister: *Materials Science and Engineering: an Introduction*, 7th ed., John Wiley and Sons Inc., New York, NY, 2007, pp. 418–24.
14. P. Kofstad: *High Temperature Oxidation of Metals*, John Wiley and Sons Inc, New York, NY, 1996, pp. 306–08.
15. L. Navais: *J. Am. Ceram. Soc.*, 1961, vol. 44 (9), pp. 434–46.
16. J.A. Ball, M. Pirzada, R.W. Grimes, M.O. Zacate, D.W. Price, and B.P. Uberuaga: *J. Phys. Condens. Matter*, 2005, vol. 17, pp. 7621–31.
17. W.F. McClune: International Diffraction File, Inorganic Volume, JCPDS International Center for Diffraction Data, 1984, vol. 4, pp. 832–33.